Proc. Natl. Acad. Sci. USA
Vol. 93, pp. 2867–2872, April 1996
Physiology

Oxygen supply and oxygen-dependent gene expression in differentiating embryonic stem cells

(embryoid bodies/hypoxia/cell viability/vascular endothelial growth factor/aldolase A)

MAX GASSMANN*†, JOACHIM FANDREY‡, SANDRINE BICHET*, MARIA WARTENBERG§, HUGO H. MARTI*, CHRISTIAN BAUER*, ROLAND H. WENGER*, AND HELMUT ACKER§

*Physiologisches Institut der Universität Zürich-Irchel, Winterthurerstrasse 190, 8057 Zurich, Switzerland; ‡Physiologisches Institut I der Universität Bonn, Nussallee 11, 53115 Bonn, Germany; §Max-Planck-Institut für Molekulare Physiologie, Rheinlanddamm 201, 44026 Dortmund, Germany

Communicated by Ewald R. Weibel, University of Bern, Bern, Switzerland, December 21, 1995 (received for review August 24, 1995)

ABSTRACT **Blastocyst-derived pluripotent mouse embryonic stem cells can differentiate *in vitro* to form so-called embryoid bodies (EBs), which recapitulate several aspects of murine embryogenesis. We used this *in vitro* model to study oxygen supply and consumption as well as the response to reduced oxygenation during the earliest stages of development. EBs were found to grow equally well when cultured at 20% (normoxia) or 1% (hypoxia) oxygen during the first 5 days of differentiation. Microelectrode measurements of pericellular oxygen tension within 13- to 14-day-old EBs (diameter 510–890 μm) done at 20% oxygen revealed efficient oxygenation of the EBs' core region. Confocal laser scanning microscopy analysis of EBs incubated with fluorescent dyes that specifically stain living cells confirmed that the cells within an EB were viable. To determine the EBs' capability to sense low oxygen tension and to specifically respond to low ambient oxygen by modulating gene expression we quantified aldolase A and vascular endothelial growth factor (VEGF) mRNAs, since expression of these genes is upregulated by hypoxia in a variety of cells. Compared with the normoxic controls, we found increased aldolase A and VEGF mRNA levels after exposing 8- to 9-day-old EBs to 1% oxygen. We propose that EBs represent a powerful tool to study oxygen-regulated gene expression during the early steps of embryogenesis, where the preimplantation conceptus resides in a fluid environment with low oxygen tension until implantation and vascularization allow efficient oxygenation.**

The first third of gestation involves extensive morphogenetic changes of the mouse embryo in which the fertilized oocyte develops to a complex embryonic structure showing signs of organ differentiation, including vascularization. From fertilization until implantation the oxygen needed for cellular metabolism is supplied by diffusion from the fluid phase within the oviduct and uterus, respectively. This implies that the early embryo is adapted to grow in an environment with reduced oxygenation until the onset of vascularization. Very little is known about the adaptation of the conceptus to this low oxygen milieu and how the oxygen tension (P_{O_2}) influences embryogenesis, since conventional studies of living embryos are hindered by their relative inaccessibility and their limited availability. However, this difficulty might be circumvented by using an *in vitro* model of murine embryogenesis. Pluripotent embryonic stem (ES) cells are derived from the inner cell mass of mouse blastocysts (1, 2) and can be propagated *in vitro* indefinitely without any genetic manipulation (3). In the absence of the leukemia inhibitory factor, normal ES cells differentiate spontaneously into three-dimensional structures termed embryoid bodies (EBs) which recapitulate several aspects of murine embryogenesis, including formation of endoderm, mesoderm and ectoderm, as well as more advanced processes such as hematopoiesis, cardiogenesis, and angiogenesis (4–9).

Oxygen is known to regulate expression of a growing number of genes such as the growth factors erythropoietin (EPO) (reviewed in ref. 10) and vascular endothelial growth factor (VEGF) (reviewed in ref. 11) as well as glycolytic enzymes (12). Oxygen-dependent regulation of gene expression has been extensively studied on the glycoprotein hormone EPO, which represents the main stimulator of erythropoiesis, and more recently on VEGF. It has been shown that this endothelial cell-specific mitogen (13, 14) is a key regulator of angiogenesis, a process which leads to the formation of new capillary sprouts from preexisting vessels (15, 16). Angiogenesis is essential in the developing embryo as well as in the adult mammal, where it exerts its function during wound healing and corpus luteum formation. Besides its physiological role, angiogenesis is also involved in pathological processes such as tumor growth (reviewed in refs. 11 and 17). Recent reports showing that the highest tumor-derived VEGF levels were found in the cells surrounding necrotic areas of glioblastomas suggested that hypoxia regulates VEGF expression (18, 19). This notion was verified by *in vitro* experiments demonstrating oxygen-dependent VEGF gene expression in malignant as well as in normal cells (20–22). Besides inducing EPO and VEGF, hypoxia has been shown to induce expression of the ubiquitous glycolytic enzymes, including fructose-1,6-bisphosphate aldolase A, phosphoglycerate kinase 1, pyruvate kinase M, and lactate dehydrogenase A (12, 23–26). During reduced oxygenation, anaerobic glycolysis represents the main energy source of the cells.

In the present study we determined oxygenation of EBs by microelectrode measurement of pericellular oxygen tension, defined the oxygen consumption, and investigated the viability of the cells within EBs by confocal laser scanning microscopy using vital dyes. To examine whether EBs are capable of sensing and responding to low oxygen, we exposed EBs to hypoxic conditions and quantified aldolase A and VEGF mRNA.

MATERIALS AND METHODS

Culture Conditions. The ES cell line CCE (27) was cultured as described previously (28). Briefly, the cells were grown on gelatin-coated dishes without feeders in Dulbecco's modified Eagle's medium supplemented with 20% fetal calf serum (Boehringer Mannheim), 1000 units of murine leukemia inhibitory factor per ml (GIBCO/BRL), 150 μM monothioglycerol, 1× minimum essential medium (MEM) nonessential

The publication costs of this article were defrayed in part by page charge payment. This article must therefore be hereby marked "*advertisement*" in accordance with 18 U.S.C. §1734 solely to indicate this fact.

Abbreviations: ES, embryonic stem; EB, embryoid body; EPO, erythropoietin; VEGF, vascular endothelial growth factor; DASPMI, 4-(4-dimethylaminostyryl)-1-methylpyridinium iodide.

†To whom reprint requests should be addressed.

amino acids, 100 units of penicillin per ml, and 0.1 mg of streptomycin per ml in a humidified atmosphere containing 5% CO_2 at 37°C, and passaged every 2–3 days. At day 0 of ES cell differentiation, trypsinized cells were seeded at 0.5–10 × 10^3 cells per ml on Petri dishes (200 μl/cm^2) in Iscove's modified Dulbecco's medium (IMDM) containing 0.9% methylcellulose (Methocel MC; Fluka), 15% fetal calf serum (HyClone), transferrin at 0.3 mg/ml, insulin at 0.01 mg/ml, 1× MEM nonessential amino acids, 450 μM monothioglycerol, and antibiotics. For cell counting, the EBs were enzymatically dissociated. Routinely, 200–900 EBs were transferred to IMDM and centrifuged at 150 × *g* for 10 min, and the pellet was incubated in 2 ml of dispase II (2.4 units/ml; Boehringer Mannheim) supplemented with 0.1 unit of collagenase per ml at 37°C for 10–30 min.

Histological Analysis of EBs. EBs were transferred to IMDM, centrifuged at 150 × *g* for 10 min, fixed in Schaffer's solution [96 ml of methanol, 50 ml of 35% (wt/vol) formaldehyde, and 4 ml of glucose/phosphate buffer (54 mM Na_2HPO_4/12 mM KH_2PO_4/155 mM glucose, pH 7.4)] for 6 h and dehydrated in 1 ml of methanol overnight. Subsequently, the EBs were embedded in JB-4 embedding medium (Polyscience), following the manufacturers directions, cut with a microtome in 3.5- to 4-μm sections, and stained with Giemsa stain.

Confocal Laser Scanning Microscopy. Vital cell staining of EBs was performed with the fluorescent dyes 4-(4-dimethylaminostyryl)-1-methylpyridinium iodide (DASPMI or 4-Di-1-ASP) or calcein AM (both from Molecular Probes). The EBs were transferred into 1 ml of Ham's F10 medium (GIBCO/BRL) and stained either with 5 μM DASPMI for 90 min at 37°C or, after the EBs had been incubated at 6–8°C for 10 min, with 20 μM calcein AM at 6–8°C for 1 h. Immediately after staining, the incubation medium was removed and the EBs were washed six times with F10 medium. Optical sectioning of EBs was performed with a confocal scanning laser setup (MCR 600, Bio-Rad) connected to an inverted microscope as described (28).

P_{O_2} Measurements and O_2 Consumption. P_{O_2} distribution profiles in EBs with diameters ranging from 510 to 890 μm were measured in a perfusion chamber at 37°C as described for tumor cell spheroids (29). To stabilize the EBs for perfusion with isotonic salt solution (Locke's solution) and insertion of the microelectrode, they were positioned on a small metal plate which contained bore holes. Single-channel microelectrodes with a tip diameter of 2–4 μm were used for polarographic P_{O_2} measurements. Two-point calibration was performed by insertion of the electrodes into the flowing medium previously equilibrated with gas mixtures containing 5% CO_2 in either air or pure nitrogen. Calibration was repeated after P_{O_2} measurements. Only results from stable electrodes were considered for subsequent evaluation. For P_{O_2} measurements inside the EBs, the microelectrode was placed in close proximity to the upper surface of the EBs with a deviation angle of 15° from the vertical axis. By using a step-driven micromanipulator, the electrode was moved in 50-μm steps toward the center of the EB. Routinely, 8–10 separate points were measured per EB.

Oxygen consumption ($\dot{V}_{O_2}$, expressed as ml of O_2 per 100 g wet weight of tissue per min) was calculated from the measured P_{O_2} profile inside the EBs as described (30, 31) by adapting Henry's law:

$$P_{O_2}(r) = P_{O_2}(s) - \dot{V}_{O_2}(6D\alpha)^{-1}(R^2 - r^2),$$

where $P_{O_2}(r) = P_{O_2}$ at r; $P_{O_2}(s) = P_{O_2}$ at the surface; D = oxygen diffusion coefficient (32); α = oxygen solubility coefficient (32); R = radius of EB; and r = distance to the center. This mathematically developed equation assumes spherical geometry of EBs and constant values for α and D. Since there are no direct determinations of D for mouse embryonic tissue, we used the D constant determined for lung tissue (32) according to Bartels (33).

Quantitation of Aldolase A and VEGF mRNA. The EBs were washed in IMDM and centrifuged at 150 × *g* for 10 min, and total RNA was isolated from the pellet according to ref. 34. Total RNA (10 μg) was denatured in formamide/formaldehyde and electrophoresed through a 1% agarose gel containing 6% formaldehyde as described (35). After pressure blotting (PosiBlot, Stratagene) to a nylon membrane (Biodyne A, Pall), followed by UV crosslinking (Stratalinker, Stratagene), the RNA was hybridized to ^{32}P-labeled probes according to the manufacturer's directions (Pall). The radioactive signal was recorded and quantified by using a PhosphorImager (Molecular Dynamics). The aldolase A probe was cloned from a HepG2 cDNA library and the β-actin cDNA was purchased from Clontech. Aldolase A and VEGF mRNA signals were normalized to the β-actin signal to correct for loading and blotting differences. The mouse VEGF probe was derived from a 644-bp PCR fragment generated by using the forward primer A (5′-GCGGGCTGCCTCGCAGTC-3′) and the reverse primer B (5′-TCACCGCCTTGGCTTGTCAC-3′), corresponding to bp 16–33 and 659–690, respectively, of the murine VEGF cDNA sequence according to ref. 36. The internal primer C (5′-GCTCACAGTGATTTTCTGGCT-3′) corresponding to bp 496–516 (36) was designed to exclusively amplify the cDNA of transcripts encoding the 164 amino acid isoform of VEGF. The competitor VEGF template was constructed exactly as described by Siebert and Larrick (37), and competitive PCR was performed using the conditions reported recently for EPO (38).

RESULTS

Differentiation of ES Cells in Normoxic and Hypoxic Conditions. EBs were obtained by culturing the feeder-independent ES cell line CCE (27) in a semisolid medium in the absence of leukemia inhibitory factor (39). In a first set of experiments, differentiating ES cells were cultured in normoxic or hypoxic conditions (20% O_2 and 1% O_2, respectively). At low oxygen tension, the plating efficiency of ES cells increased 2-fold, while the average number of cells forming an EB was not altered within the first 5 days of EB differentiation (data not shown). This observation is in agreement with recent reports demonstrating a favorable effect on plating efficiency and hematopoietic differentiation when oxygenation of differentiating EB cells is reduced (40, 41). However, further cultivation of EBs at 1% O_2 after 5 days resulted in a decreasing number of viable EBs. To optimize plating efficiency and provide favorable growing conditions, the ES cells were grown at 1% O_2 for 3 days, changed to 4% O_2 for an additional 4 days, and switched to 20% O_2 until the EBs were analyzed. Under these culture conditions, the average EB consisted of about 10^4 cells at differentiation day 13–14.

Viability of the Cells Within the EBs. Large regions of dead cells are always observed in the central region of growing multicellular spheroids derived from tumor cells (42). However, cell viability inside developing EBs is a prerequisite for an *in vitro* model of embryogenesis. To test whether this requirement was fulfilled, sections of 6- to 8-day-old EBs with diameters of about 250–400 μm were Giemsa stained and analyzed by light microscopy. As exemplified in Fig. 1*A*, the EB's structure consisted of loosely associated cells and showed regions of beginning cavities. Although no signs of cell death were observed, we were mindful that histological studies have a limited ability to determine cell viability. To assess vital cell function more accurately, developing EBs were incubated with the fluorescent dyes DASPMI or calcein AM, which specifically stain living cells. The isomeric styryl dye DASPMI is a specific vital stain for mitochondria; DASPMI uptake is a

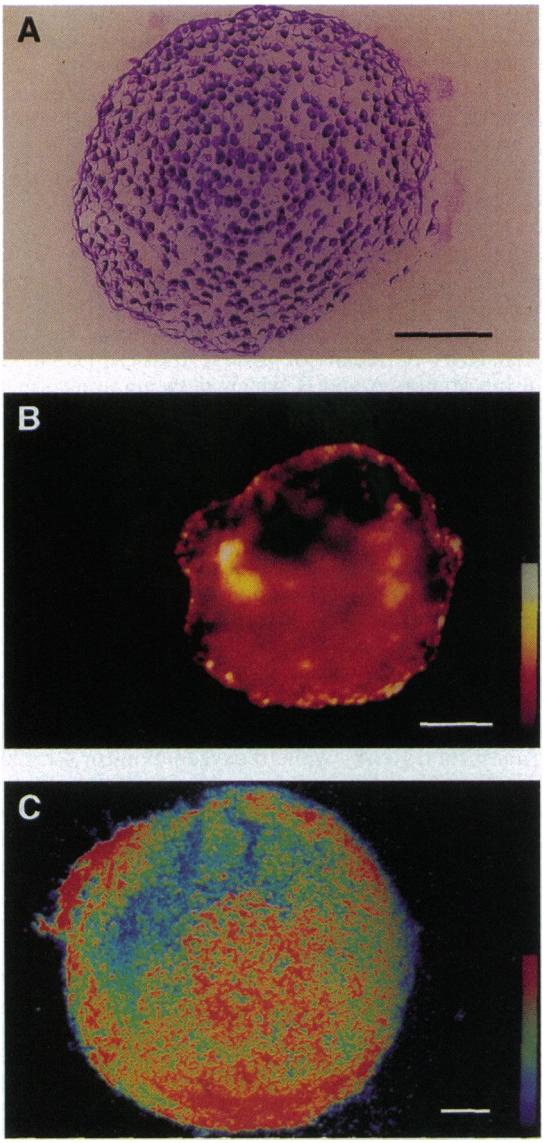

FIG. 1. Histological and confocal laser scanning microscopy analysis of EBs. After 7 days of differentiation, EBs were stained either with Giemsa stain for histological analysis (*A*) or with the vital dye DASPMI for confocal laser scanning microscopy (*B*). Fluorescence intensity at the equatorial plane is coded in pseudocolors ranging from high levels (yellow) to low levels (dark red). At differentiation day 13, calcein AM-stained EBs were mechanically sectioned in the equatorial plane prior to analysis (*C*). The pseudocolors range from high levels (red) to low levels (dark blue). (Bars = 100 μm.)

function of membrane potential, and its fluorescence intensity is a measure for mitochondrial energization (43). On the other hand, the lipophilic dye calcein AM passively crosses the cell membrane and is subsequently converted by cellular esterases to a polar fluorescent product which is retained in the cytoplasm of living cells with intact membranes (44).

In situ analysis of the fluorescent stained cells or tissues can be facilitated by the application of confocal laser scanning microscopy, which allows optical sectioning of a discrete slice of about 10 μm within the intact specimen (45). Fluorescent cells beyond the focused section as well as nonfluorescent cells are not visible (46). At day 7 of differentiation, five DASPMI-stained EBs were analyzed for cellular vitality. Optical sectioning of EBs scanned at the equatorial plane and visualized with pseudocolors revealed a heterogenous distribution of fluorescence within the whole EB, as exemplified in Fig. 1*B* (diameter of the EB, 330 μm). To determine their vitality during further development, 13- to 14-day-old EBs (n = 9) were incubated with calcein AM. Fig. 1*C* shows an example of one EB mechanically sectioned in the equatorial plane since penetration of the scanning laser is limited to a depth of about 250 μm (47). As in Fig. 1*B*, accumulation of the dye was observed throughout the whole EB, although the intensity was not uniformly distributed. This finding can be explained by the fact that with advanced stages of differentiation EBs, like embryos, show regions of high cell density (e.g., myocardial cells) as well as formation of cavities (4–9). Low fluorescence intensity due to dead cells rather than to cavitation can be excluded by our previous observation in which the lethal dye Lucifer yellow/VS was used to visualize dying or dead cells: EBs did not show the necrotic areas which were prominent in tumor cell-derived spheroids (28). Taken together, our data strongly support the idea that the cells inside the EBs are viable.

Oxygen Supply and Consumption Within EBs. The observation that the EB-forming cells were viable even in the core region of the EBs suggested an efficient oxygen supply through the outer cell layer into the center part of each EB. Fig. 2*A* summarizes the P_{O_2} values measured at 20% O_2 in 16 EBs at differentiation day 13–14 with a diameter ranging from 510 to 890 μm. Indeed, measurements of pericellular oxygen tension within single EBs revealed only a moderate decrease in P_{O_2} when a microelectrode was moved in 50-μm steps from the surface toward the core region. For every single point measured within the EB (8–10 points per EB) we calculated oxygen

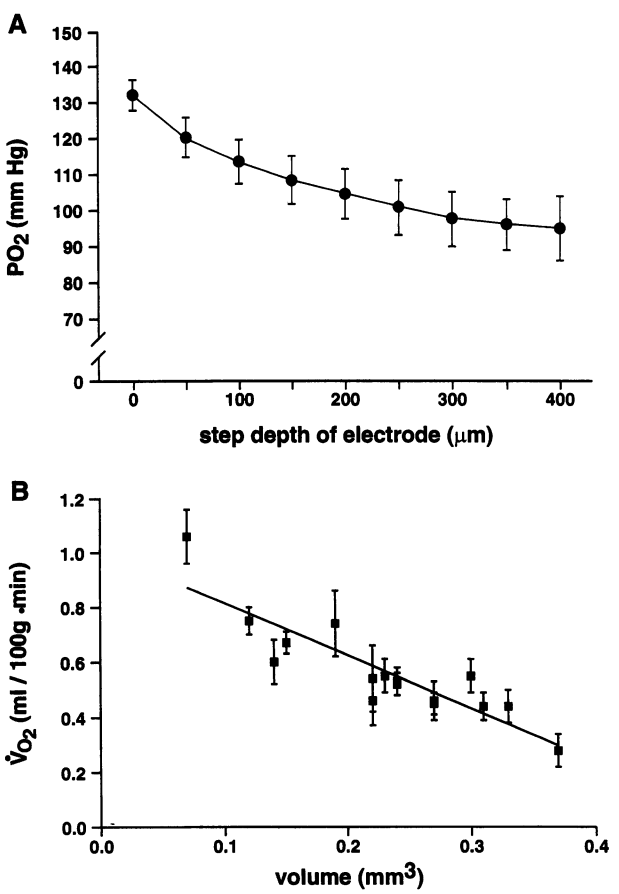

FIG. 2. P_{O_2} profile and oxygen consumption inside EBs. One mmHg = 133 Pa. (*A*) A total of 129 P_{O_2} values from 16 EBs at differentiation day 13–14 (diameter: 510–890 μm) were measured at 20% oxygen by using a P_{O_2} microelectrode, which was moved from the periphery (0 μm) toward the center of the EB. Values are given as mean ± SD. (*B*) Oxygen consumption within EBs as a function of their volume was calculated from the recorded P_{O_2} values. Correlation coefficient: −0.91 ($P < 0.001$).

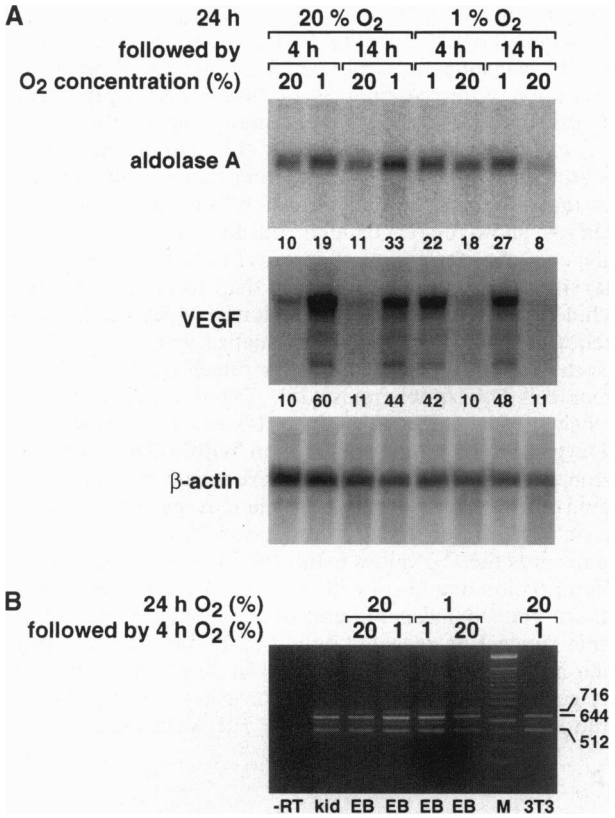

FIG. 3. Analysis of aldolase A and VEGF mRNA. EBs 8–9 days old were preincubated at 20% or 1% oxygen prior to exposure for 4 and 14 h at the indicated oxygen concentration. (*A*) Quantitative Northern blot analysis of aldolase A and VEGF mRNA. Each lane was loaded with 10 μg of total RNA isolated after stimulation. After electrophoresis and blotting, the membrane was hybridized to probes encoding aldolase A, VEGF, and β-actin. The signals for aldolase A and VEGF were quantified by PhosphorImager analysis and corrected for differences in loading and blotting by normalization to the signal obtained with the β-actin probe. The normalized values are indicated below each lane. (*B*) Reverse transcriptase-mediated PCR analysis of VEGF mRNA was performed with 1 μg of total RNA from EBs using primers A and B. Samples (1 μg) of total RNA isolated from kidney (kid) and NIH 3T3 fibroblasts (3T3) were used as positive controls. −RT, reverse transcriptase omitted; M, DNA migration of a 100-bp ladder (Pharmacia). Numbers on right are cDNA product lengths in bp.

consumption ($\dot{V}_{O_2}$), thus representing the integral from $r = 0$ to $r = R$ (see *Materials and Methods*). Within an EB, the standard deviation was ≤10% of the mean value, indicating similar $\dot{V}_{O_2}$ values throughout the EB. In Fig. 2*B*, the mean oxygen consumption measured in 16 EBs is plotted versus their respective volumes. As expected from the homogeneous P_{O_2} gradients in EBs of different sizes (Fig. 2*A*), EBs with the largest volume had the lowest oxygen consumption.

Oxygen-Dependent Regulation of Aldolase A and VEGF mRNA. To analyze whether EBs were able to adapt to hypoxic conditions by specifically upregulating oxygen-dependent genes encoding glycolytic enzymes, we investigated modulation of the ubiquitously expressed aldolase A. Total RNA was isolated from 8-day-old EBs that were exposed either to normoxia for 1 day followed by an additional hypoxic (1% O_2) incubation for a further 4 and 14 h or to hypoxia for 1 day followed by an additional incubation at normoxic conditions for 4 and 14 h. Northern blot analysis revealed an up to 3-fold reversible hypoxic induction of aldolase A mRNA regardless of which hypoxic induction protocol was performed (Fig. 3*A*). This observation implies that EBs are metabolically active and have the capability of upregulating glycolytic activity under reduced oxygenation. Our results are in agreement with a previous report showing a 2- to 5-fold induction of aldolase A mRNA after hypoxic induction of skeletal muscle cells (12).

To test whether oxygen also influences expression of genes involved in the regulation of embryonic development, we sought to study hypoxic induction of VEGF, since expression of this potent inducer of angiogenesis was expected to occur in EBs. Indeed, Northern blot analysis showed that VEGF mRNA was present in normoxic EBs and that the mRNA level was reversibly increased by a factor of 4–6 when EBs were exposed to hypoxia (Fig. 3*A*). Similar to induction of aldolase A, elevation of VEGF mRNA was independent of the chosen hypoxic induction scheme (see above). Since splicing events are known to result in different VEGF isoforms, we analyzed total EB RNA by means of reverse transcriptase-mediated PCR using primers A and B, which allow amplification of the complete coding region (see *Materials and Methods*). As shown in Fig. 3*B*, three different cDNA products, 512, 644, and 716 bp in length, were obtained that correspond to the 120-, 164-, and 188-amino acid isoforms of mature VEGF, respectively (48). Interestingly, hypoxic induction of all three isoforms was about equal. Since the amplified product encoding the 164-amino acid form was the most abundant one, we quantitated this isoform by means of competitive PCR using the primer set A and C, which exclusively amplifies this form. EBs grown at 20% oxygen contained 6 amol of VEGF mRNA per μg of total RNA, whereas exposure at 1% oxygen for 4 h induced VEGF mRNA levels to 34 amol/μg of total RNA. EBs preincubated at 1% oxygen for 24 h still had markedly high VEGF levels (17 amol/μg of total RNA), while reoxygenation for 4 h reduced the VEGF mRNA level to 2 amol/μg of total RNA. The induction factor of the 164-amino acid isoform after hypoxic exposure very closely resembled the one obtained from all VEGF isoforms as measured by Northern blot analysis (see above). In conclusion, these results demonstrate that growing EBs have the capability to sense changes in their ambient oxygen tension and to respond to them by modulation of gene expression.

DISCUSSION

The potential of ES cells to spontaneously differentiate *in vitro* into embryo-like structures has facilitated developmental studies of the peri-implantation mouse embryo. However, although cell death occurs in the center of tumor cell-derived multicellular spheroids, little is known about the viability of the differentiating cells within the forming EBs. In the present work we stained 7- and 13-day-old EBs with the fluorescent dyes DASPMI and calcein AM, which stain living cells by different mechanisms. Subsequent analysis by confocal laser scanning microscopy showed no signs of cell death within the growing EBs, implying an efficient oxygenation of the EBs. Indeed, the P_{O_2} values in the core region of the EBs were surprisingly high compared with measurements performed on different tumor cells in multicellular spheroid culture showing central P_{O_2} values close to zero (42, 49). In contrast to similar-sized EBs analyzed in this work, we have observed significant areas of necrosis in the central region of multicellular spheroids starting at a spheroid diameter of about 300 μm (47). The differences between these three-dimensional tissue culture models might be explained by the about 10 times higher cell packing density of tumor cell-derived spheroids compared with our similar-sized EBs: when reaching a diameter of 800 μm, spheroids derived from HepG2 cells or human malignant gliomas consisted of about 7 and 12 × 10^4 cells, respectively (50). Thus, increased cell number and metabolism of the tumor cells most probably result in steeper P_{O_2} gradients, causing a higher susceptibility to cell death. This is compatible with the appearance of anoxic and necrotic areas in fast-growing tumors *in vivo* if angiogenesis cannot keep pace with the increase in tumor mass (11, 17). In striking contrast to tumor growth, our measurements provide evidence that EBs, which are

composed of "normal" differentiating cells, can grow beyond a certain size and stay fully viable throughout the whole core region. A prerequisite for efficient oxygenation is a shallow P_{O_2} gradient such as we have recorded from all of our EBs. In this respect, efficient oxygenation of EBs seems to adequately recapitulate the *in vivo* situation of a developing blastula which also experiences low P_{O_2} values as determined for the uterus in rats (51) and hamsters (52). We propose that exposure of EBs to conditions with P_{O_2} values comparable to those that have been measured *in vivo* in the reproductive tract would still result in a sufficiently high P_{O_2} in the EB core region. Calculation of the oxygen consumption revealed that the shallow P_{O_2} gradients for all different sizes of EBs appear to be the result of low oxygen consumption: EBs with the largest volume displayed the lowest oxygen consumption rate at all depths, and that consumption was markedly lower than in tumor spheroids of comparable size (taking into consideration equal values for D and α according to ref. 30). Decreasing oxygen consumption with increasing volume has already been observed in tumor cell spheroids (30) and can be explained by a change from oxidative to glycolytic metabolism. The resulting shallow decrease in the P_{O_2} throughout the EBs from the periphery to the core region still provided a mean P_{O_2} of 95 mmHg even at 400 μm of depth. The regulatory mechanisms that allow adaptation of the oxygen consumption rate to the EBs' size still remain to be elucidated. Since larger EBs utilize less oxygen even in their outer cell layers, it is unlikely that a limitation in O_2 availability accounts for the reduced consumption rate. Interestingly, calculation of the maximal tissue volume in which an early mouse embryo *ex vivo* can be oxygenated by diffusion only revealed a diameter of about 700 μm, assuming a spherical embryo, a maternal P_{O_2} of 75 mmHg and an embryonic $\dot{V}_{O_2}$ of 1.3 ml of O_2 per 100 g wet weight per min (33). Thus, the EBs in culture seem to have an oxygenation profile similar to that of the early mouse embryo.

High cell viability and favorable effects of hypoxia on plating efficiency and hematopoietic differentiation encouraged us to test whether EBs are able to respond to hypoxia by upregulating gene expression. We showed that hypoxic exposure of EBs led to a 3-fold accumulation of aldolase A mRNA. Since induction of glycolytic enzymes facilitates ATP production in the cell through anaerobic glycolysis, hypoxic upregulation of aldolase A demonstrates the EBs' capability to adapt to reduced oxygenation. Apart from aldolase A, we showed that mRNA from the angiogenic growth factor VEGF, which is known to be regulated in an oxygen-dependent manner, was present in 8- to 9-day-old EBs. This result is in agreement with a previous report showing that EBs induce vascular sprouting of host endothelial cells when grafted onto quail chorioallantoic membrane (6). Furthermore, *in vitro* formation of vascular channels has been described in growing EBs (7, 9), and the addition of recombinant VEGF to a chemically defined medium containing bone morphogenetic protein 4 (BMP-4) but not fetal bovine serum (53) led to an increase in expression of the endothelial cell marker *flk-1* in EBs after 5 days of culture (M. V. Wiles, personal communication). VEGF is thought to be the central mediator of embryonic vasculogenesis and angiogenesis (48, 54). Since its expression is most probably upregulated by local hypoxic conditions within the developing embryo, we postulate that the increase in VEGF mRNA found after lowered oxygen supply of EBs mimics the *in vivo* situation during embryonic blood vessel formation. As EBs are known to express several growth factors and their receptors (55), the favorable effects of hypoxia on plating efficiency and hematopoietic differentiation of EBs might reflect increased expression of oxygen-regulated growth factors, including VEGF, EPO, acidic/basic fibroblast growth factor, and platelet-derived growth factor (56), as well as cytokines such as interleukin 6 (57) and interleukin 8 (58).

We propose that low oxygen consumption of the cells within an EB allows the EBs to grow in a poorly oxygenated environment. This might reflect the *in vivo* situation, where the preimplantation mammalian conceptus resides in a fluid environment sharing no physical connection with the maternal organism. Therefore, survival of the embryo depends on the availability of oxygen and nutrients in the environment. Interestingly, oxygen tension in the mammalian reproductive tract has been reported to be much less than half that of atmospheric oxygen, ranging from high values of about 60 mmHg (8.7% atmospheric O_2) in the oviduct and uterus of hamsters and rabbits to as low as 11 mmHg (1.5% O_2) in the uterus of rhesus monkeys (59). In hamster and rabbits, intrauterine oxygen concentrations further decreased during blastulation and implantation to 37 mmHg (5.3% O_2) and 24 mmHg (3.5% O_2), respectively. The significance of reduced intrauterine oxygen tension at the time of implantation is unknown. Besides the hypothesis that this mechanism may serve to protect the peri-implantation embryo from oxygen toxicity (59), it is tempting to speculate that hypoxia represents a physiological stimulus during development: reduced oxygen supply of the preimplantation embryo might be a prerequisite to upregulate a specific set of genes needed during the earliest steps of development, while, after implantation and vascularization, expression of these genes might be either reduced to constitutive levels or turned off. In summary, we propose that EBs provide an *in vitro* model to study oxygen-regulated gene expression during the earliest steps of mammalian embryogenesis such as formation of endoderm, mesoderm, and ectoderm.

We thank W. Baier-Kustermann and G. Holtermann for superb technical assistance, R. Rüegg for histological analysis of the EBs, M. V. Wiles and J. Silke for helpful suggestions and critical reading of the manuscript, C. Eberhard for preparation of the manuscript, and C. Gasser for the art work. This project was supported by grants from the Swiss National Science Foundation (31-36369.92 to M.G.), the Deutsche Forschungsgemeinschaft (Ac37/9-1), and the Deutsche Krebshilfe (w49/91/Acl) as well as by the Hartmann Müller-Stiftung and by a fellowship from the Bonizzi-Theler Stiftung to S.B.

1. Evans, M. J. & Kaufman, M. H. (1981) *Nature (London)* **292,** 154–156.
2. Martin, G. R. (1981) *Proc. Natl. Acad. Sci. USA* **78,** 7634–7638.
3. Robertson, E. J. (1987) in *Teratocarcinomas and Embryonic Stem Cells: A Practical Approach*, ed. Robertson, E. J. (IRL, Oxford), pp. 71–112.
4. Doetschman, T. C., Eistetter, H., Katz, M., Schmidt, W. & Kemler, R. (1985) *J. Embryol. Exp. Morphol.* **87,** 27–45.
5. Hooper, M. L. (1992) *Embryonal Stem Cells* (Harwood Academic, Chur, Switzerland).
6. Risau, W., Sariola, H., Zerwes, H.-G., Sasse, J., Ekblom, P., Kemler, R. & Doetschman, T. (1988) *Development (Cambridge, U.K.)* **102,** 471–478.
7. Wang, R., Clark, R. & Bautch, V. L. (1992) *Development (Cambridge, U.K.)* **114,** 303–316.
8. Doetschman, T., Shull, M., Kier, A. & Coffin, D. (1993) *Hypertension* **22,** 618–629.
9. Young, P. E., Baumhueter, S. & Lasky, L. A. (1995) *Blood* **85,** 96–105.
10. Jelkmann, W. (1992) *Physiol. Rev.* **72,** 449–489.
11. Plate, K. H., Breier, G. & Risau, W. (1994) *Brain Pathol.* **4,** 207–218.
12. Webster, K. A. (1987) *Mol. Cell. Biochem.* **77,** 19–28.
13. Leung, D. W., Cachianes, G., Kuang, W. J., Goeddel, D. V. & Ferrara, N. (1989) *Science* **246,** 1306–1309.
14. Keck, P. J., Hauser, S. D., Krivi, G., Sanzo, K., Warren, T., Feder, J. & Connolly, D. T. (1989) *Science* **246,** 1309–1312.
15. Risau, W. (1990) *Prog. Growth Factor Res.* **2,** 71–79.
16. Folkman, J. & Shing, Y. (1992) *J. Biol. Chem.* **267,** 10931–10934.
17. Folkman, J. (1995) *Nat. Med.* **1,** 27–32.
18. Plate, K. H., Breier, G., Weich, H. A. & Risau, W. (1992) *Nature (London)* **359,** 845–848.
19. Shweiki, D., Itin, A., Soffer, D. & Keshet, E. (1992) *Nature (London)* **359,** 843–845.

20. Goldberg, M. A. & Schneider, T. J. (1994) *J. Biol. Chem.* **269,** 4355–4359.
21. Minchenko, A., Bauer, T., Salcenda, S. & Caro, J. (1994) *Lab. Invest.* **71,** 374–379.
22. Levy, A. P., Levy, N. S., Wegner, S. & Goldberg, M. A. (1995) *J. Biol. Chem.* **270,** 13333–13340.
23. Semenza, G. L., Roth, P. H., Fang, H.-M. & Wang, G. L. (1994) *J. Biol. Chem.* **269,** 23757–23763.
24. Firth, J. D., Ebert, B. L., Pugh, C. W. & Ratcliffe, P. J. (1994) *Proc. Natl. Acad. Sci. USA* **91,** 6496–6500.
25. Marti, H. H., Jung, H. H., Pfeilschifter, H. & Bauer, C. (1994) *Eur. J. Physiol.* **429,** 216–222.
26. Firth, J. D., Ebert, B. L. & Ratcliffe, P. J. (1995) *J. Biol. Chem.* **270,** 21021–21027.
27. Robertson, E., Bradley, A., Kuehn, M. & Evans, M. (1986) *Nature (London)* **323,** 445–448.
28. Gassmann, M., Wartenberg, M., McClanahan, T., Fandrey, J., Bichet, S., Kreuter, R., Acker, H. & Bauer, C. (1995) *Toxicol. in Vitro* **9,** 429–438.
29. Görlach, A., Holtermann, G., Jelkmann, W., Hancock, J. T., Jones, S. A., Jones, O. T. G. & Acker, H. (1993) *Biochem. J.* **190,** 771–776.
30. Schwachöfer, J. H. M., Acker, H., Crooijmans, R. P. M. A., Holtermann, G., Hoogenhout, J., Kal, H. B. & Theeuwes, A. G. M. (1992) *Cancer Res. Ther. Control* **3,** 7–14.
31. Grossmann, U. (1984) *Recent Results Cancer Res.* **95,** 150–161.
32. Grote, J. (1967) *Pflügers Arch.* **195,** 245–254.
33. Bartels, H. (1970) *Prenatal Respiration* (North-Holland, Amsterdam), pp. 1–14.
34. Chomczynski, P. & Sacchi, N. (1987) *Anal. Biochem.* **162,** 156–159.
35. Sambrook, J., Fritsch, E. F. & Maniatis, T. (1989) *Molecular Cloning: A Laboratory Manual* (Cold Spring Harbor Lab. Press, Plainview, NY).
36. Claffey, K. P., Wilkison, W. O. & Spiegelman, B. M. (1992) *J. Biol. Chem.* **267,** 16317–16322.
37. Siebert, P. D. & Larrick, J. W. (1992) *Nature (London)* **359,** 557–558.
38. Fandrey, J. & Bunn, H. F. (1993) *Blood* **81,** 617–623.
39. Wiles, M. V. & Keller, G. (1991) *Development (Cambridge, U.K.)* **111,** 259–267.
40. Wiles, M. V. (1993) *Methods Enzymol.* **225,** 900–918.
41. Potocnik, A. J., Nielsen, P. J. & Eichmann, K. (1994) *EMBO J.* **13,** 5274–5281.
42. Sutherland, R. M. (1988) *Science* **240,** 177–184.
43. Bereiter-Hahn, J., Seipel, K.-H., Vöth, M. & Ploem, J. S. (1983) *Cell Biochem. Funct.* **1,** 147–155.
44. Morris, S. J. (1990) *BioTechniques* **8,** 296–308.
45. Pawley, J. B. (1990) *Handbook of Biological Confocal Microscopy* (Plenum, New York).
46. Cross, A. R., Henderson, L., Jones, O. T. G., Delpiano, M. A., Hentschel, J. & Acker, H. (1990) *Biochem. J.* **272,** 743–747.
47. Wartenberg, M. & Acker, H. (1995) *Micron*, in press.
48. Breier, G., Albrecht, U., Sterrer, S. & Risau, W. (1992) *Development (Cambridge, U.K.)* **114,** 521–532.
49. Görlach, A. & Acker, H. (1994) *Biochim. Biophys. Acta* **1227,** 105–112.
50. Görlach, A., Bölling, B., Holtermann, G., Schwachöfer, J. H. M., Carlsson, J. & Acker, H. (1995) *Int. Oncol.* **7,** 831–839.
51. Mitchell, J. A. & Yochim, J. M. (1968) *Endocrinology* **83,** 691–705.
52. Kaufman, D. L. & Mitchell, J. A. (1994) *Comp. Biochem. Physiol. A* **107,** 673–678.
53. Johansson, B. M. & Wiles, M. V. (1995) *Mol. Cell. Biol.* **15,** 141–151.
54. Millauer, B., Shawver, L. K., Plate, K. H., Risau, W. & Ullrich, A. (1994) *Nature (London)* **367,** 576–579.
55. Schmitt, R. M., Bruyns, E. & Snodgrass, H. R. (1991) *Genes Dev.* **5,** 728–740.
56. Kuwabara, K., Ogawa, S., Matsumoto, M., Koga, S., Clauss, M., Pinsky, D. J., Lyn, P., Leavy, J., Witte, L., Joseph-Silverstein, J., Furie, M. B., Torica, G., Cozzolino, F., Kamada, T. & Stern, D. M. (1995) *Proc. Natl. Acad. Sci. USA* **92,** 4606–4610.
57. Yan, S. F., Tritto, I., Pinsky, D., Liao, H., Huang, J., Fuller, G., Brett, J., May, L. & Stern, D. (1995) *J. Biol. Chem.* **270,** 11463–11471.
58. Karakurum, M., Shreeniwas, R., Chen, J., Pinsky, D., Yan, S.-D., Anderson, M., Sunouchi, K., Major, J., Hamilton, T., Kuwabara, K., Rot, A., Nowygrod, R. & Stern, D. (1994) *J. Clin. Invest.* **93,** 1564–1570.
59. Fischer, B. & Bavister, B. D. (1993) *J. Reprod. Fertil.* **99,** 673–679.